Electrochimica Acta 527 (2025) 146232

Contents lists available at ScienceDirect

Electrochimica Acta

journal homepage: www.journals.elsevier.com/electrochimica-acta

Electrochemical reduction mechanism of 4-nitrobenzyl bromide in ionogel membranes

Tehreema Naeem, Silvia Mena, Jordi Hernando, Gonzalo Guirado *

Departament de Química, Universitat Autònoma de Barcelona 08193, Bellaterra, Barcelona, Spain

ARTICLE INFO

Keywords:
Green electrolytes
Ionic liquids
Ionogel membranes
Electrosynthesis

ABSTRACT

Ionic liquid-based electrolytes (ILs) have gained tremendous attention as sustainable, green electrolytes for electrochemical processes due to their negligible vapour pressure and high boiling points. A rising trend is to fabricate solid electrolytes based on ionic liquids to address the risk of leakage associated to liquid electrolytes. These solid electrolytes, which are commonly known as ionogel membranes (IGs), contain the intrinsic properties of ILs, while having excellent mechanical strength. These characteristics make them ideal for investigating reaction mechanisms and facilitating electrosynthesis processes. By providing a stable and conductive environment, ionogels enable precise control and monitoring of electrochemical reactions in solid electrolytes, leading to more accurate and reproducible results. Their application not only enhances our understanding of fundamental electrochemical processes but also paves the way for innovative advancements in electrosynthesis, contributing significantly to the development of new materials and technologies. In this body of research, the reduction mechanism of *p*-nitrobenzyl bromide (*p*-NBBr) is studied and disclosed in IG membranes for a first time. We successfully performed a controlled potential electrolysis of *p*-NBBr in IG membranes, as well as studying two different electrochemical setups to obtain the most optimal configuration. We also demonstrate that the addition of electrolyte additives, such as lithium bis(trifluorometahnesulfonyl)imide (Li TFSI), in the IG composition raises the ionic conductivity of the resulting membrane from 0.15 up to 0.2 mS/cm.

1. Introduction

Nitrobenzyl halides have been the focus of numerous electrochemical studies over the years. Reductive cleavage of their C-X bond provides ample opportunities for organic synthesis, such as for the preparation of organometallic compounds and dimer products and is also a model for studying intramolecular electron transfer processes [1–4]. The electrochemical reduction mechanism of halogenated organic compounds in organic solvents has been well documented. The recognized mechanism begins with the first electron transfer to form an anion radical, followed by bond cleavage of the C-X bond to form a radical intermediate, which can then be coupled to provide a dimerized product following an EC (Electrochemical-Chemical) mechanism or can be further reduced to a carbanion, leading mainly to nitrotoluene, following an ECE (Electrochemical-Chemical-Electrochemical) mechanism [5–7].

Solvents and electrolytes play critical roles in electrosynthesis. An electrolyte medium consisting of a solvent and a supporting electrolyte is essential for all electrochemical reactions. Most electrochemical studies have been performed in conventional organic solvents such as acetonitrile (ACN) and dimethyl sulfoxide (DMSO), which are one of the main causes of waste in synthesis and environmental degradation due to their volatile nature. It has been reported that extensive use of organic solvents generates about 80 % waste leading to environmental pollution, energy consumption, and higher resource wastage. There is a major drive towards more green and sustainable solvents [8,9]. Some of the strategies for more sustainable synthesis are the use of benign solvents such as water, supercritical CO_2, and ionic liquids [10–12].

Ionic liquids or room temperature ionic liquids (RTILs) are, in general, a class of salts that are liquids below 100 °C and have excellent thermal and chemical stability. ILs have irregular structures with large organic cations and organic or inorganic anions. These structural features disfavour compact molecular packing and result in a very low melting point and low lattice energy. ILs generally have high boiling points, low vapour pressures, high flame slowing down, and from moderate-to-high ionic conductivities (generally spanning from 1.0 mS/cm to 10.0 mS/cm) [13–16]. Conventional organic electrolyte solutions used for electrochemical purposes include the use of high concentrations

* Corresponding author.
E-mail address: gonzalo.guirado@uab.cat (G. Guirado).

https://doi.org/10.1016/j.electacta.2025.146232
Received 27 February 2025; Received in revised form 9 April 2025; Accepted 13 April 2025
Available online 14 April 2025

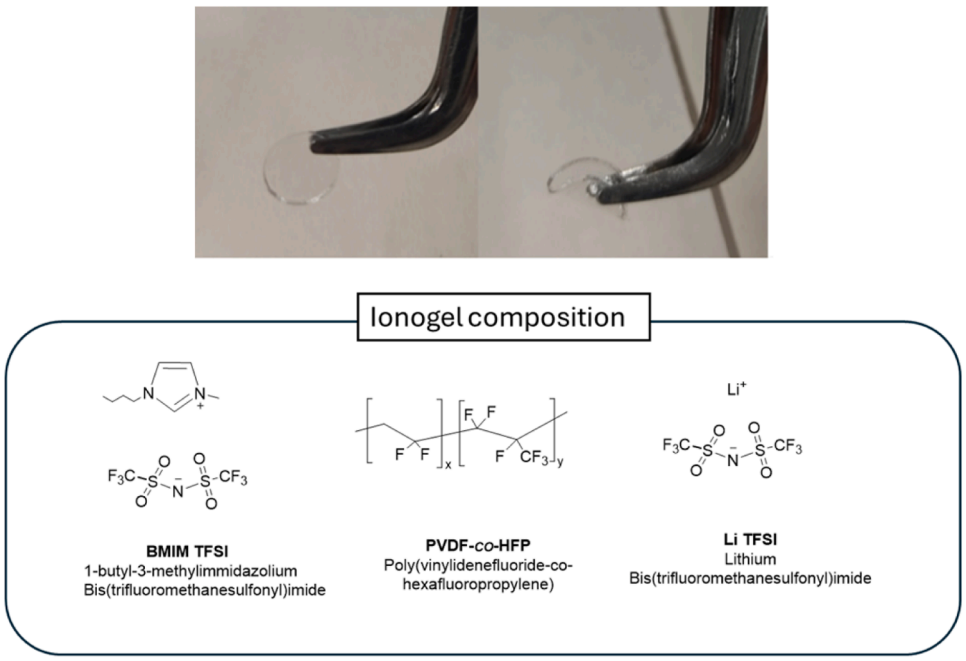

Fig. 1. (Up) Ionogel membrane. (Bottom) Chart of structures of BMIM TFSI, PVDF-co-HFP, and Li TFSI.

of supporting electrolytes. ILs as an electrolyte medium can act as both solvent and supporting electrolyte simultaneously due to their inherent conductive nature. There have been several recent reports of the use of ILs to conduct electrochemical studies effectively instead of conventional electrolyte solutions such as imidazolium-based ILs as electrolytes for high-energy green supercapacitors and lithium-sulphur batteries [17–22].

Despite having several excellent properties as electrolytes, ILs fall short due to their liquid nature, which implies a risk of leakage and consequent prevention of their use in practical, long-term applications [23,24]. To avoid this limitation, they can be synthesized into a quasi-solid class of electrolytes known as ionogel membranes. In IGs a dispersed IL phase is immobilized in a continuous solid matrix to obtain a gel-like material, which has the intrinsic physicochemical properties of ILs in combination with the mechanical strength caused by the solid matrix eliminating the problem of outflow [25–29]. IG-based electrolytes have been extensively investigated in the last decade for use as electrolytes in lithium batteries, solid-state superconductors, and sensors [30–34]. However, neither the disclosure of electrochemical reaction mechanisms nor electrosynthetic processes has been reported up to now.

These features make them perfect for studying reaction mechanisms and supporting electrosynthesis processes. By offering a stable and conductive setting, ionogels allow for precise control and observation of electrochemical reactions, resulting in more accurate and consistent outcomes. Their application not only deepens our understanding of basic electrochemical processes but also fosters innovative progress in electrosynthesis, significantly aiding the development of new materials and technologies.

For this reason, this work presents the electrochemical reduction of a nitrobenzyl halide, *p*-nitrobenzyl bromide (*p*-NBBr), in IG membranes, as quasi-solid electrolyte media for a first time as a model process, optimising the membrane composition for performing the electrochemical reduction process. Besides, IG membranes are explored as sustainable alternatives for reaction electrolytes in electrosynthesis, offering several significant advantages in terms of conductivity, stability, versatility as well as environmental benefits showing the recyclability of this kind of membranes.

2. Experimental section

2.1. Materials and reagents

p-Nitrobenzyl bromide (99 %), *p*-nitrotoluene (*p*-NT, 99 %), and poly (vinylidene fluoride-*co*-hexafluoropropylene) (PVDF-*co*-HFP), and tetrabutylammonium hexafluorophosphate (TBA PF_6, for electrochemical analysis, ≥ 99.0 %) were purchased from Merck and used as received. *p, p*'-dinitrobibenzyl was purchased from Molekula and used without further purification. High-purity acetonitrile was purchased from Acros Organics (> 99.5 %). The ionic liquid 1-butyl-3-methylimidazolium bis (trifluoromethanesulfonyl)imide (BMIM TFSI) was purchased from Solvionic and used without further purification. Li TFSI was purchased from Sigma-Aldrich (purity ≥ 99.0 %) and used as received.

2.2. Preparation of IG membranes

For *p*-NBBr-loaded IG membranes, PVDF-*co*-HFP (0.23 g) and BMIM TFSI (0.8 mL) were mixed in a 1:5 wt ratio. 5 mL of acetone were added to the mixture and left to stir overnight at room temperature until the polymer pellets were completely dissolved. Then the desired amount of *p*-NBBr was dissolved into de IG solution mixture and was stirred until it was completely dissolved. After adding *p*-NBBr to the mixture, 90 μL of IG solution was poured into a poly(dimethylsiloxane) (PDMS)–based silicone template and left to air-dry for 15–20 min. As a result, free-standing and elastic 1 cm diameter solid membranes were obtained of ~200 μm of thickness (Fig. 1). For increasing ionic conductivity in the membranes, Li TFSI was added to the membranes, obtaining ionogels with a composition of 10 wt. % PVDF-*co*-HFP, 10 wt. % Li TFSI and 80 wt. % BMIM TFSI.

2.3. Characterization techniques

Cyclic voltammetry (CV) was used for electrochemical characterizing *p*-NBBr in the different electrolytic media. For ACN/0.1 M TBA PF_6 and BMIM TFSI solvents, cyclic voltammetry experiments were performed in a three-electrode system with glassy carbon ($\phi = 1$ mm) as the working electrode (WE). A Pt disk ($\phi < 1$ mm) was used as the counter electrode (CE) along with a saturated calomel electrode (SCE) as the

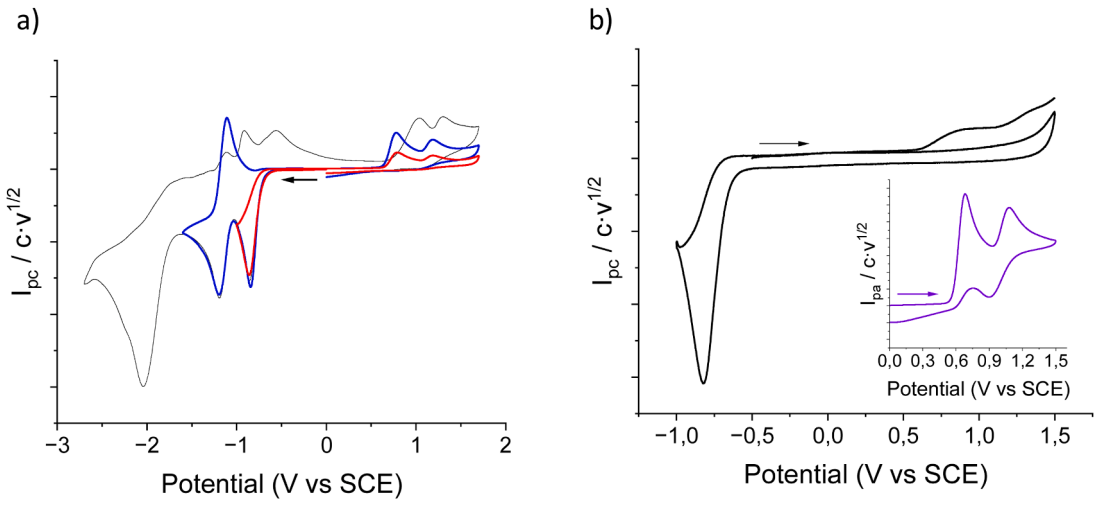

Fig. 2. (a) Cyclic voltammograms of p-NBBr ($c = 15$ mM) in ACN/0.1 M TBA PF_6 (b) Cyclic voltammogram of p-NBBr ($c = 15$ mM) in ACN/ 0.1 M $TBAPF_6$, focusing on only the first reduction electron transfer. (inset) CV of tetraethylammonium bromide (TEA Br, $c = 10$ mM) solution in ACN/0.1 M TBA PF_6. Arrows in (a) and (b) indicate the direction of the potential scan in each case. WE GC, CE Pt and RE SCE, scan rate 0.1 V/s.

reference electrode (RE). All the potentials given in this work are referenced to this electrode. CV measurements were recorded on the Model 660E Potentiostat CHInstrument. For controlled-potential electrolysis, experiments were performed at room temperature with constant Ar gas purging. A graphite rod was used as the working electrode with a Pt bar and SCE as counter and reference electrodes, respectively. The reference electrode isolated from the working electrode compartment by a salt bridge. The salt solution of the reference calomel electrode is separated from the electrochemical solution by a salt-bridge ended with a frit, which is made of a ceramic material, allowing ionic conduction between the two solutions and avoiding appreciable contamination. Ideally, the electrolyte solution present in the bridge is the same as the one used for the electrochemical solution, in order to minimise junction potentials. The error associated with the potential values is <5 mV.

Regarding the IG membranes, CV and AC impedance spectroscopy (EIS) analyses were conducted using a three-electrode system based on screen-printed commercial electrodes from Methrom DropSens. The DRP-110 three-electrode system selected had working and counter electrodes made of carbon vitreous and a silver pseudo-reference electrode. The diameter of the working electrode was 4 mm. For AC impedance analysis, the testing frequency was set between 1 Hz to 100 KHz with 5 mV of amplitude for both samples. These measurements were recorded on the Model 660E Potentiostat CHInstrument and impedance spectra were fitted with CHI660E software to calculate the ionic conductivity of the membranes. In order to improve the control potential electrolysis in IGs membranes, a two-electrode system based on two foils of Cu in a sandwich configuration were used.

In addition, all the currents were normalized and they are given as a current function ($I_p/c{\cdot}v^{1/2}$).

IG film thickness was examined by means of confocal imaging as a non-contact optical 3D profiling technique using a DCM 3D optical profilometer (Leica).

All products obtained, and the commercial analogues were characterised by ^{1}H NMR. Measurements were made using a Bruker DPX400 (400 MHz) (Billerica, MA, USA) spectrometer. Proton chemical shifts were reported in ppm (d) ($CDCl_3$, δ=7.26, or CD_3CN, δ=1.94). The J values are reported in Hz.

Table 1
Electrochemical parameters of the cyclic voltammograms of *p*-NBBr ($c = 15$ mM) in ACN + 0.1 M $TBAPF_6$ at 25 °C.

scan rate (V/s)	E_{pc} (V vs SCE) [a]	ΔE_p (mV)[b]	n°. of electrons[c]
0.05	−0.84	75	1.0_6
0.1	−0.85	72	1.1_3
0.2	−0.86	73	1.0_8
0.3	−0.87	74	1.1_0
0.5	−0.88	70	1.1_7
0.7	−0.88	72	1.2_0

[a] Peak potential of the first cathodic peak. [b] $\Delta E_p = |E_{pc} - E_{pc/2}|$. [c] Number of electrons transferred for the first cathodic peak, which was determined by comparison with a redox probe under the same experimental conditions.

3. Results and discussion

3.1. Electrochemical reduction mechanism of p-NBBr in conventional electrolytic media

First, the electrochemical behaviour of *p*-NBBr in acetonitrile (+ 0.1 M TBA PF_6, as supporting electrolyte) was established using CV on glassy carbon as a working electrode (Fig. 2a). The cathodic scan, up to -2.7 V (vs SCE), shows three different electron transfers. First, a fast electron transfer at −0.84 V (vs SCE), followed by a second reversible electron transfer at −1.18 V (vs SCE), and a third multi-electron irreversible cathodic wave at −2.36 V (vs SCE), which corresponds to the reduction of the nitroso group of the molecule. It is possible to detect the formation of nitroso derivatives due to the appearing of new oxidation peaks at $E_{pa} = -0.91$ V (vs SCE) and $E_{pa} = -0.54$ V (vs SCE) in the anodic counter scan [35,36]. However, the current study will focus only on the first electron transfer (Fig. 2b), which electrochemical parameters where summarized in Table 1.

According to the electrochemical characterization performed, *p*-NBBr anion radical is formed after the first electron transfer (electrochemical reaction (E)) corresponding to the 1 electron irreversible reduction wave at −0.84 V (vs SCE), which is confirmed by other studies reported [37–38]. Considering the irreversible nature of the reduction wave, it is presumed that the formed anion radical would evolve following a bond-breaking cleavage reaction (first-order chemical reaction, C) after intramolecular electron transfer from the nitro group to the C-Br bond, leading to the formation of a *p*-nitrobenzyl radical and a bromide anion. This conclusion was supported by the observation of the subsequent oxidation peak at +0.80 V (vs SCE), which can be attributed

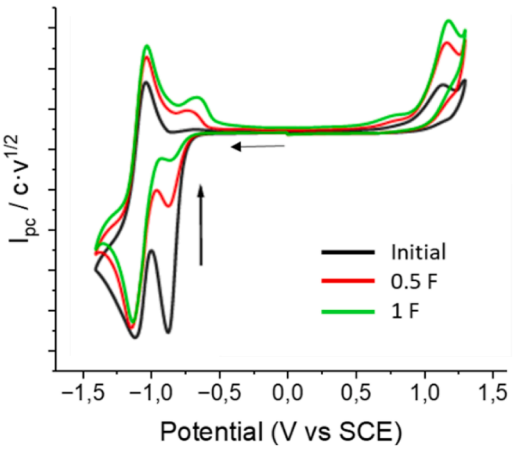

Fig. 3. Cyclic voltammograms monitorization of *p*-NBBr CPE in ACN/0.1 M TBA PF_6.

to the oxidation wave of the Br^- anion formed. In fact, we could confirm this assignment by recording the cyclic voltammogram of tetraethylammonium bromide, whose anion gave the same oxidation peak at +0.80 V (vs SCE) (inset in Fig. 2b).

To determine the nature of the electrochemically formed product after the first reduction electron transfer, controlled-potential electrolysis (CPE) was used and tracked with cyclic voltammetry. CPE was performed for the acetonitrile solution of *p*-NBBr, after first reduction peak, at E_{ap} = −0.95 V (vs SCE), and cyclic voltammograms were recorded to monitor the electrolysis process (Fig. 3). After passing 1 F of current, the solution turned from transparent to pale yellow, indicating the formation of a new product.

The product was extracted from the resulting solution and, after subsequent analysis by ^{1}H NMR, it could be identified as *p,p*'-dinitrobibenzyl, which had been obtained electrochemically in 95 % yield. In view of this, we could propose a one-electron EC reduction mechanism for the reduction of *p*-NBBr followed by a dimerization reaction, as established from the electrochemical data (Scheme 1) [36].

3.2. Electrochemical reduction mechanism of p-NBBr in BMIM TFSI

Next, cyclic voltammetry was used to characterise the electrochemical reduction of *p*-NBBr in BMIM TFSI, a common ionic liquid which will be based the IG membrane. The electrochemical parameters were summarized in Table 2. Similar results to those previously measured in ACN were obtained, registering a fast irreversible monoelectronic electron transfer (E_{pc} = −0.81 V (vs SCE)) followed by a reversible electron transfer (E_{pc} = −1.10 V (vs SCE)) in the initial cathodic scan (Fig. 4). The dependence of the peak current and potential values with the scan rate followed the same behaviour previously established in ACN, which allowed us to assume that *p*-NBBr should also undergo an EC reduction mechanism in BMIM TFSI leading to C-Br bond breaking.

To know the nature of the product obtained, a controlled potential electrolysis of a *p*-NBBr solution in BMIM TFSI was performed after first electron transfer, at E_{ap} = −0.95 V (vs SCE), and after the passage of 1F and a chemical treatment of the electrolysed sample, ^{1}H NMR analysis revealed the presence of the expected p,p'-dinitrobibenzyl product with a yield of 56 %, and a 44 % of the unreacted starting material (p-NBBr). This result confirmed that *p*-NBBr also follows an EC reaction in BMIM TFSI after one-electron reduction, which leads to the formation of the *p*-

Table 2
Electrochemical parameters of the cyclic voltammograms of p-NBBr (*c* = 15 mM) in BMIM TFSI at 25 °C.

scan rate (V/s)	E_{pc} (V)[a]	ΔE_{pc} (mV)[b]	N°. of electrons[c]
0.05	−0.78	74	1.0_6
0.1	−0.81	68	1.0_7
0.2	−0.82	68	1.0_3
0.3	−0.83	68	1.0_1
0.5	−0.84	71	1.0_1
0.7	−0.85	74	1.0_0

[a] Peak potential of the first cathodic peak. [b] $\Delta E_p = |E_{pc} - E_{pc/2}|$. [c] Number of electrons transferred for the first cathodic peak, which was determined by which was determined by comparison with a redox probe under the same experimental conditions.

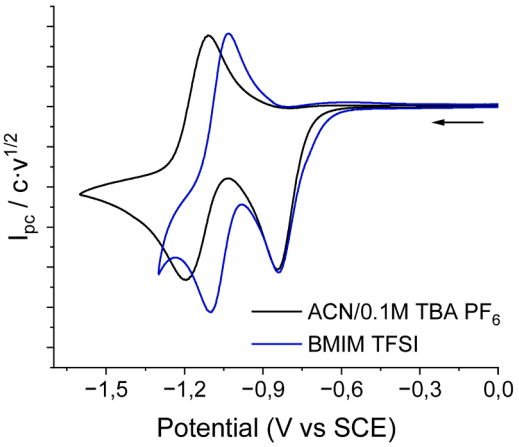

Fig. 4. Comparison between cyclic voltammograms of p-NBBr (*c* = 15 mM) in BMIM TFSI and ACN/0.1 M TBA PF_6. (WE = GC, CE = Pt and RE = SCE; scan rate 0.1 V/s).

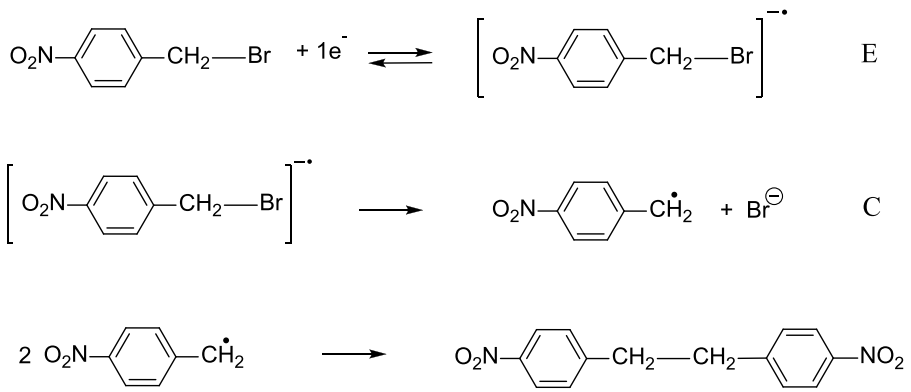

Scheme 1. EC reduction mechanism proposed for p-NBBr, which leads to p,p'-dinitrobibenzyl formation via radical dimerization.

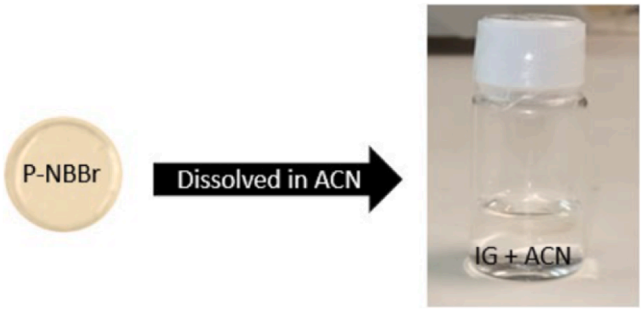

Fig. 5. (a) Schematic representation of solid IG membranes to solution (b) CV of p-NBBr IG membrane dissolved in ACN + 0.1 M TBA PF_6. (WE = GC, CE = Pt and RE = SCE; scan rate 0.1 V/s).

nitrobenzyl radical after electroinduced C-Br cleavage that eventually undergoes dimerization to generate the *p,p'*-dinitrobibenzyl product (see Scheme 1 above).

3.3. Electrochemical reduction of p-NBBr in ionogel membranes

It was evaluated the electrochemical behaviour of *p*-NBBr in ionogel membranes, which are IL-based solid electrolytes. For IG preparation, PVDF-*co*-HFP was used as the continuous solid polymer phase that was swollen with BMIM TFSI. For this reason, we first analysed whether PVDF-*co*-HFP could affect the electrochemical performance of *p*-NBBr, for which we conducted CV and CPE experiments in an ACN (+ 0.1 M $TBAPF_6$) solution in which it was dissolved an ionogel (Fig. 5). As expected, similar results to those previously measured in the absence of the dissolved polymer were observed. Thus, a fast irreversible monoelectronic electron transfer was found to occur at $E_{pc} = -0.87$ V (vs SCE) by CV, while exhaustive bulk electrolysis led to the major formation of *p,p'*-dinitrobibenzyl (40 % Yield). Hence, we did not observe any significant effect of polymer addition on the electrochemical behaviour of *p*-NBBr, except for a slight decrement of the coupled chemical reaction that can be attributed to the increased viscosity of the medium caused by dissolving PVDF-*co*-HFP.

After establishing the negligent character of PVDF-*co*-HFP into the solution, *p*-NBBr-loaded IG membranes of 230 μm thickness were fabricated with a 1:5 polymer/BMIM TFSI weight ratio ($c_{p\text{-NBBr}} = 10$ mM in the IL phase) and were characterized by means of CV. However, cyclic voltammograms obtained did not reproduce the behaviour previously observed in liquid solution; instead, ill-defined reduction waves were measured at lower potentials (Fig. 6a). As this result could not be enhanced by increasing the concentration of *p*-NBBr, we attributed it to the slow ion diffusion within the IG membranes caused by the continuous solid polymer matrix surrounding the IL domains. Consequently, this should lead to low ionic conductivities for these materials. It is important to highlight that no release or leakage of the IL from the membrane was detected after performing the electrochemical experiments.

To overcome this limitation, a dopant salt (Li TFSI) was added to the IG membranes to increase their ionic conductivity, which was quantified using EIS (Fig. 6b). A clear increase in ionic conductivity from 0.15 mS/cm to 0.19 mS/cm was observed in this way for the Li TFSI-containing membrane. Fig. 6b showed how the cyclic voltammogram of the IG enhance its electrochemical response, observing the two expected reduction waves for *p*-NBBr that resemble those previously measured with liquid electrolytes.

In view of these results, we postulated that the same EC reduction mechanism of *p*-NBBr previously established in liquid electrolytes should also be operating in IG membranes despite their lower ionic conductivity. Thus, it was conducted a control potential electrolysis of *p*-NBBr on the IG membranes placed on SPE electrode at an applied potential of −0.95 V (vs Ag) for 1F. Then, the membrane was dissolved in ACN, and the products generated were extracted with mixtures of toluene/water and identified by ^{1}H NMR analysis, which confirmed the formation of *p,p'*-dinitrobibenzyl (Table 3, entry 1). It must be noted that the time required for the exhaustive electrolysis of *p*-NBBr in the IG membranes was much larger than for analogous experiments conducted in liquid electrolytes, increasing the electrolysis time from <1 h up to 4 h when the CPE was stopped. This means that, despite adding Li TFSI, the electron-transfer kinetics in IGs and, therefore, the resulting electrochemical reaction are significantly slower, which we ascribe to the slow diffusion of ions in the membranes as well as to the poor contact

Table 3
Results of electrochemical reduction of p-NBBr in IG membranes.

Entry	Electrode	E_{ap} (V)	Time for 1F	Yield *p,p'*-dinitrobibenzyl (%)	Selectivity (%)
1	3-Electrode System, SPE	−0.95 V (vs Ag)	4 h	22	100
2	2-Electrode system, Cu foils	−1.1 V (vs Cu)	1 h	24	100

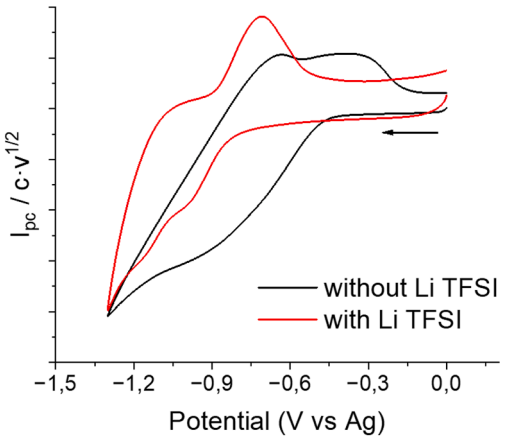

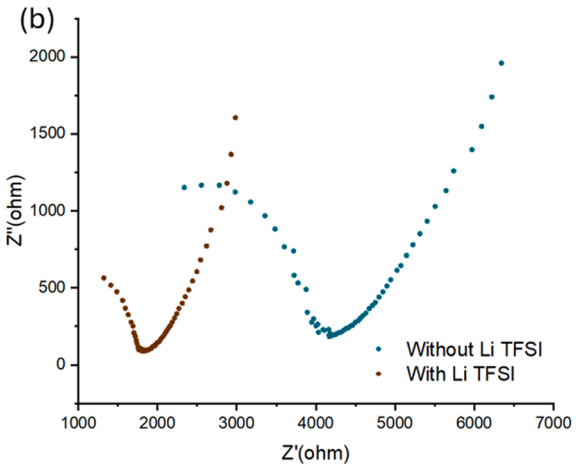

Fig. 6. (a) Cyclic voltammograms of p-NBBr in PVDF-co-HFP/BMIM TFSI IG membranes with and without the addition of Li TFSI (WE and CE = screen-printed vitreous carbon, RE = screen-printed silver; scan rate: 0.1 V/s). (b) Electrochemical impedance spectra of the p-NBBr/PVDF-co-HFP/BMIM TFSI IG membranes with and without added Li TFSI.

between the electrode surface and membranes. The latter is even further aggravated by the screen-printed three-electrode system used to conduct the electrolysis experiments, where only one of the faces of the membranes was in contact with a 4 mm-in-diameter WE.

To avoid this issue, exhaustive controlled electrolysis experiments were performed with a different electrochemical setup to increase the efficiency of the reaction. For this, we moved from a three-electrode to two-electrode system consisting of two Cu strips sandwiching the solid IG membrane. In this case, a control potential electrolysis was performed at $E_{ap} = -1.1$ V (vs Cu) for 1F. After treatment of the electrolysed membrane and ^{1}H NMR analysis, major transformation of *p*-NBBr into *p,p'*-dinitrobibenzyl was confirmed after only 1 h (Table 3, entry 2).

Therefore, in both cases *p,p'*-dinitrobibenzyl was obtained as a unique product of an electrochemical reduction reaction in a quasi-solid electrolyte media with high selectivity. The lower yield obtained in IG membranes compared to conventional organic electrolyte media is due to the mass transfer process. In IG membranes, the reactant only reaches the electrode surface by diffusion (with a diffusion coefficient of approximately 10^{-11} m^2/s for *p*-NBBr), whereas in organic electrolytes, mass transport is mainly by convection. If the experiment is performed discontinuously, allowing the material at the electrode surface to be renewed, it is expected to achieve the same yield values since the electrochemical reaction is completely selective. Finally, it is important to note that the membranes can be recycled and reused after each electrosynthesis. Recyclability studies conducted with the IG membranes revealed that a recovery of ca. 85 % can be achieved after 4 cycles without any loss of the physicochemical properties of the membrane.

4. Conclusions

In summary, the reductive electrosynthesis of *p,p'*-dinitrobibenzyl was analysed in different electrolytic media: organic solvents with supporting electrolytes, ionic liquids, and polymer ionogels. An EC-based electrochemical mechanism was established for the reduction of *p*-NBBr in all these media, which resulted in the formation of *p*-nitrobenzyl radicals through electroinduced C-Br cleavage that eventually dimerised to produce *p,p'*-dinitrobibenzyl. To ensure this process to occur in ionogels, membranes were prepared by combining the fluorinated copolymer PVDF-*co*-HFP with the ionic liquid BMIM TFSI and adding Li TFSI as a dopant salt. The latter allowed increasing ionic conductivity without affecting the EC reaction mechanism. To the best of our knowledge, this is the first report of the use of IG membranes as reaction media in the performance of sustainable electrosynthesis. Based on all the preceding results, IG membranes could be an effective and environmentally friendly replacement for the aprotic reaction media typically used for electrosynthesis.

Declaration of competing interest

The authors declare that there are no conflicts to declare.

Acknowledgments

The authors also thank the Ministerio de Ciencia e Innovación of Spain for financial support through project PID2022–141293OB-I00 and TED2021-130797B-I00 (MICIU/AEI/10.13039/ 501100011033 and ERDF - A way of making Europe). In addition, the authors thank AGAUR (Generalitat de Catalunya, 2021 SGR 00052 and 2021 SGR 00064). As well, this work is part of the research conducted within the E3tech+ network RED2022–134552-T, funded by MCIU/AEI/10.13039/ 501100011033. T.N. thanks to the Generalitat de Catalunya (AGAUR) for a FI-SDUR PhD fellowship 2023F1SDU-00069. S.M. acknowledges support from the postdoctoral grant Juan de la Cierva JDC2022–048606-I, funding by MCIN/AEI/10.13039/501100011033 and the European Union "NextGenerationEU"/PRTR.

References

[1] C.P. Andrieux, J.-M. Savéant, K.B. Su, Kinetics of dissociative electron transfer. Direct and mediated electrochemical reductive cleavage of the carbon-halogen bond, J. Phys. Chem. 90 (1986) 3815–3823, https://doi.org/10.1021/j100407a059.
[2] J.P. Bays, S.T. Blumer, S. Baral-Tosh, D. Behar, P. Neta, Intramolecular electron transfer and dehalogenation of nitroaromatic anion radicals, J. Am. Chem. Soc. 105 (1983) 320–324, https://doi.org/10.1021/ja00341a003.
[3] D.E. Bartak, M.D. Hawley, Stabilities of the anion radicals of nitrobenzyl derivatives, J. Am. Chem. Soc. 94 (1972) 640–642, https://doi.org/10.1021/ja00757a058.
[4] M. Mohammad, A single two electron transfer or high disproportionation: electrochemical reduction of dinitrobibenzyl, Electrochim. Acta 22 (1977) 487–488, https://doi.org/10.1016/0013-4686(77)85105-0.
[5] L. Álvarez-Griera, I. Gallardo, G. Guirado, Estimation of nitrobenzyl radicals reduction potential using spectro-electrochemical techniques, Electrochim. Acta 54 (2009) 5098–5108, https://doi.org/10.1016/j.electacta.2009.02.037.
[6] H.D. Burrows, E.M. Kosower, Optical spectra and reactivities of radical anions of 4-nitrobenzyl compounds produced by pulse radiolysis of acetonitrile solutions, J. Phys. Chem. 78 (1974) 112–117, https://doi.org/10.1021/j100595a006.
[7] E. Norambuena, C. Olea, C. Aliaga, Cyclic voltammetry and electron paramagnetic resonance study of the electrochemical reduction of P-nitrobenzyl bromide in aprotic solvents, Spectrosc. Letters 26 (1993) 1547–1557, https://doi.org/10.1080/00387019308011633.
[8] B.H. Lipshutz, F. Gallou, S. Handa, Evolution of solvents in organic chemistry, ACS. Sustain. Chem. Eng. 4 (2016) 5838–5849, https://doi.org/10.1021/acssuschemeng.6b01810.
[9] F. Gao, R. Bai, F. Ferlin, L. Vaccaro, M. Li, Y. Gu, Replacement strategies for non-green dipolar aprotic solvents, Green Chem. 22 (2020) 6240–6257, https://doi.org/10.1039/D0GC02149K.
[10] S.P. Nalawade, F. Picchioni, L.P.B.M. Janssen, Supercritical carbon dioxide as a green solvent for processing polymer melts: processing aspects and applications, Progr. Poly. Sci. (Oxford) 31 (2006) 19–43, https://doi.org/10.1016/J.PROGPOLYMSCI.2005.08.002.
[11] H.J. Lehmler, Synthesis of environmentally relevant fluorinated surfactants–a review, Chemosphere 58 (2005) 1471–1496, https://doi.org/10.1016/j.chemosphere.2004.11.078.
[12] S.A. Forsyth, J.M. Pringle, D.R. MacFarlane, Ionic liquids – an overview, Aust. J. Chem. 57 (2004) 113–119, https://doi.org/10.1071/CH03231.
[13] E. Kianfar, S. Mafi, Ionic liquids: properties, application, and synthesis. Fine chemical engineering, Fine Chem. Eng. 2 (2020) 21–29, https://doi.org/10.37256/fce.212021693.
[14] J.O. Valderrama, R.E. Rojas, Critical properties of ionic liquids, Revisited, Ind. Eng. Chem. Res. Industri. Eng. Chem. Res. 48 (2009) 6890–6900, https://doi.org/10.1021/ie900250g.
[15] U. Domańska, Solubilities and thermophysical properties of ionic liquids, Pure Appl. Chem. 77 (2005) 543–557, https://doi.org/10.1351/pac200577030543.
[16] M.C. Buzzeo, R.G. Evans, R.G. Compton, Non-haloaluminate room-temperature ionic liquids in electrochemistry—a review, Chemphyschem. 5 (2004) 1106–1120, https://doi.org/10.1002/cphc.200301017.
[17] L. Yu, G.Z. Chen, Ionic liquid-based electrolytes for supercapacitor and supercapattery, Front. Chem. 7 (2019) 1–15, https://doi.org/10.3389/fchem.2019.00272.
[18] N. Patil, M. Aqil, A. Aqil, F. Ouhib, R. Marcilla, Integration of redox-active catechol pendants into poly(ionic liquid) for the design of high-performance lithium-ion battery cathodes, Chem. Mater. 30 (2018) 5831–5835, https://doi.org/10.1021/acs.chemmater.8b02307.
[19] R. Thangavel, A.G. Kannan, R. Ponraj, V. Thangavel, D.W. Kim, Y.S. Lee, High-energy green supercapacitor driven by ionic liquid electrolytes as an ultra-high stable next-generation energy storage device, J. Power. Sources. 383 (2018) 102–109, https://doi.org/10.1016/j.jpowsour.2018.02.037.
[20] J.W. Park, K. Ueno, N. Tachikawa, K. Dokko, M. Watanabe, Ionic liquid electrolytes for lithium–Sulfur batteries, J. Phys. Chem. 117 (2013) 20531–20541, https://doi.org/10.1021/jp408037e.
[21] A. Fernicola, B. Scrosati, H. Ohno, Potentialities of ionic liquids as new electrolyte media in advanced electrochemical devices, Ionics. (Kiel) 12 (2006) 95–102, https://doi.org/10.1007/s11581-006-0023-5.
[22] E. Jónsson, Ionic liquids as electrolytes for energy storage applications – a modelling perspective, Energy Stor. Mater. 25 (2020) 827–835, https://doi.org/10.1016/j.ensm.2019.08.030.
[23] N. Chen, H. Zhang, L. Li, R. Chen, S. Guo, Ionogel electrolytes for high-performance lithium batteries: a review, Adv. Energy Mater. 8 (2018) 1–27, https://doi.org/10.1002/aenm.201702675.
[24] J.W. Suen, N.K. Elumalai, S. Debnath, N.M. Mubarak, C.I. Lim, M.M. Reddy, The role of interfaces in ionic liquid-based hybrid materials (Ionogels) for sensing and energy applications, Adv. Mater. Interf. 9 (2022) 1–35, https://doi.org/10.1002/admi.202201405.
[25] X. Fan, S. Liu, Z. Jia, J.J. Koh, J.C.C. Yeo, C.G. Wang, N.E. Surat'man, X.J. Loh, J. Le Bideau, C. He, Z. Li, T.P. Loh, Ionogels: recent advances in design, material properties and emerging biomedical applications, Chem. Soc. Rev. 52 (2023) 2497–2527, https://doi.org/10.1039/d2cs00652a.
[26] C.C. Yan, W. Li, Z. Liu, S. Zheng, Y. Hu, Y. Zhou, J. Guo, X. Ou, Q. Li, J. Yu, L. Li, M. Yang, Q. Liu, F. Yan, Ionogels: preparation, properties and applications, Adv. Funct. Mater. 34 (2024) 1–28, https://doi.org/10.1002/adfm.202314408.

[27] L. Zhang, D. Jiang, T. Dong, R. Das, D. Pan, C. Sun, Z. Wu, Q. Zhang, C. Liu, Z. Guo, Overview of ionogels in flexible electronics, Chem. Record 20 (2020) 948–967, https://doi.org/10.1002/tcr.202000041.
[28] Z. Luo, W. Li, J. Yan, J. Sun, Roles of ionic liquids in adjusting nature of ionogels: a mini review, Adv. Funct. Mater. 32 (2022) 1–21, https://doi.org/10.1002/adfm.202203988.
[29] D.R. MacFarlane, M. Forsyth, E.I. Izgorodina, On the concept of ionicity in ionic liquids, Phys. Chem. Chem. Phy. 11 (2009) 4962–4967, https://doi.org/10.1039/B900201D.
[30] B. Asbani, C. Douard, T. Brousse, J.Le Bideau, High temperature solid-state supercapacitor designed with ionogel electrolyte, Energy Stor. Mater. 21 (2019) 439–445, https://doi.org/10.1016/j.ensm.2019.06.004.
[31] D. Kim, G. Lee, D. Kim, J.S. Ha, Air-stable, high-performance, flexible microsupercapacitor with patterned ionogel electrolyte, ACS. Appl. Mater. Interf. 7 (2015) 4608–4615, https://doi.org/10.1021/am5077843.
[32] W.J. Hyun, C.M. Thomas, M.C. Hersam, Nanocomposite ionogel electrolytes for solid-State rechargeable batteries, Adv. Energy Mater. 10 (2020) 1–7, https://doi.org/10.1002/aenm.202002135.
[33] D.H. Cho, K.G. Cho, S. An, M.S. Kim, H.W. Oh, J. Yeo, W.C. Yoo, K. Hong, M. Kim, K.H. Lee, Self-healable, stretchable, and nonvolatile solid polymer electrolytes for sustainable energy storage and sensing applications, Energy Stor. Mater. 45 (2022) 323–331, https://doi.org/10.1016/j.ensm.2021.11.047.
[34] L. Sun, H. Huang, Q. Ding, Y. Guo, W. Sun, Z. Wu, M. Qin, Q. Guan, Z. You, Highly transparent, stretchable, and self-healable ionogel for multifunctional sensors, triboelectric nanogenerator, and wearable fibrous electronics, Adv. Fiber. Mater. 4 (2022) 98–107, https://doi.org/10.1007/s42765-021-00086-8.
[35] S. Mena, C. Loault, V. Mesa, I. Gallardo, G. Guirado, Electrochemical reduction of 4-nitrobenzyl phenyl thioether for activation and capture of CO_2, ChemElectroChem. 8 (2021) 1–14, https://doi.org/10.1002/celc.202100329.
[36] I. Gallardo, A.B. Gómez, G. Guirado, A. Lariño, M. Moreno, M. Ortigosa, S. Soler, From 4-nitrotoluene and 4,4′-dinitrobibenzyl to E-4,4′-dinitrostilbene: an electrochemical approach, New. J. Chem. 42 (2018) 7005–7015, https://doi.org/10.1039/C8NJ00131F.
[37] R.K. Norris, S.D. Barker, P. Neta, Steric effects on rates of dehalogenation of anion radicals derived from substituted nitrobenzyl halides, J. Am. Chem. Soc. 106 (1984) 3140–3144, https://doi.org/10.1021/ja00323a013.
[38] J.M. Miller, H. Pobiner, A spectrophotometric study of the reactions of p-nitrotoluene in basic solution, Anal. Chem. 36 (1964) 238–239, https://doi.org/10.1021/ac60207a004.